www.nature.com/aps

Acta Pharmacologica Sinica

ARTICLE

Betulinic acid hydroxamate prevents colonic inflammation and fibrosis in murine models of inflammatory bowel disease

María E. Prados[1], Adela García-Martín[1], Juan D. Unciti-Broceta[1], Belén Palomares[2,3,4], Juan A. Collado[2,3,4], Alberto Minassi[5], Marco A. Calzado[2,3,4], Giovanni Appendino[5] and Eduardo Muñoz[2,3,4]

Intestinal fibrosis is a common complication of inflammatory bowel disease (IBD) and is defined as an excessive accumulation of scar tissue in the intestinal wall. Intestinal fibrosis occurs in both forms of IBD: ulcerative colitis and Crohn's disease. Small-molecule inhibitors targeting hypoxia-inducing factor (HIF) prolyl-hydroxylases are promising for the development of novel antifibrotic therapies in IBD. Herein, we evaluated the therapeutic efficacy of hydroxamate of betulinic acid (BHA), a hypoxia mimetic derivative of betulinic acid, against IBD in vitro and in vivo. We showed that BAH (5–20 μM) dose-dependently enhanced collagen gel contraction and activated the HIF pathway in NIH-3T3 fibroblasts; BAH treatment also prevented the loss of trans-epithelial electrical resistance induced by proinflammatory cytokines in Caco-2 cells. In two different murine models (TNBS- and DSS-induced IBD) that cause colon fibrosis, oral administration of BAH (20, 50 mg/kg·d, for 17 days) prevented colon inflammation and fibrosis, as detected using immunohistochemistry and qPCR assays. BAH-treated animals showed a significant reduction of fibrotic markers (Tnc, Col1a2, Col3a1, Timp-1, α-SMA) and inflammatory markers (F4/80$^+$, CD3$^+$, Il-1β, Ccl3) in colon tissue, as well as an improvement in epithelial barrier integrity and wound healing. BHA displayed promising oral bioavailability, no significant activity against a panel of 68 potential pharmacological targets and was devoid of genotoxicity and cardiotoxicity. Taken together, our results provide evidence that oral administration of BAH can alleviate colon inflammation and colitis-associated fibrosis, identifying the enhancement of colon barrier integrity as a possible mechanism of action, and providing a solid rationale for additional clinical studies.

Keywords: inflammatory bowel disease; colon inflammation; fibrosis; betulinic acid hydroxamate; hypoxia-inducible factor; prolyl hydroxylases; TNBS; DSS

Acta Pharmacologica Sinica (2021) 42:1124–1138; https://doi.org/10.1038/s41401-020-0497-0

INTRODUCTION

Inflammatory bowel disease (IBD) affects millions of people worldwide and can occur with two distinct pathologies, Crohn's disease (CD) and ulcerative colitis (UC); both forms are characterized by chronic inflammation of the gastrointestinal tract, alternation of relapse and remission periods [1], and frequent development of complications such as fibrosis [2] and anemia [3].

Intestinal fibrosis is the result of chronic, recurrent or unresolved intestinal inflammation. This impaired tissue damage and reconstitution, resulting in excessive extracellular matrix (ECM) deposition and loss of normal function [4]. In UC, intestinal fibrosis is restricted to the mucosal and submucosal layers, but in CD, it can involve the entire width of the bowel wall, causing the formation of strictures. Some degree of mild to moderate fibrosis is an ordinary event in IBD that does not necessarily manifest clinically. This limited fibrosis contrasts with the severe version observed in approximately 30% of patients with CD, a high proportion of whom require surgery [5]. Importantly, intestinal fibrosis is a consequence of chronic inflammation. Over a decade following the initial diagnosis of pure inflammatory CD, up to one-third of patients then develop a stricturing or penetrating disease phenotype. Despite major therapeutic advances in the treatment of CD, the incidence of stricture formation has not markedly changed [6]. This implies that control of inflammation alone does not necessarily affect the associated fibrogenic process, whose management is still largely unmet by our current therapeutic options based on anti-inflammatory drugs (mesalamine and corticosteroids [7]), immunosuppressor drugs (azathioprine and methotrexate [8]), or, more recently, humanized monoclonal anti-TNF-α antibodies [9]. This therapeutic gap provided a rationale for investigating agents that can specifically affect the fibrotic process, such as hypoxia mimetic agents.

In this context, we have focused on the pentacyclic dietary triterpenoid betulinic acid (BA), whose pleiotropic bioactivity profile, resulting from a combination of anti-inflammatory and antioxidant properties, seemed to be of particular relevance. Thus, BA has been reported to show antinociceptive and colitis-suppressing activities [10] and a profile complementary to the

[1]Emerald Health Biotechnology, Cordoba, Spain; [2]Maimonides Biomedical Research Institute of Cordoba, Cordoba, Spain; [3]Department of Cellular Biology, Physiology and Immunology, University of Cordoba, Cordoba, Spain; [4]University Hospital Reina Sofia, Cordoba, Spain and [5]Department of Drug Science, University of Piemonte Oriental, Novara, Italy

Correspondence: Eduardo Muñoz (fi1muble@uco.es)

Received: 28 April 2020 Accepted: 29 July 2020
Published online: 18 August 2020

current therapies for IBD, but its low solubility and oral bioavailability [11–13] have thus far prevented additional development. To improve the efficacy of BA against fibrosis associated with IBD, various derivatives were prepared and assayed for their capacity to activate the hypoxia-inducing factor (HIF) pathway [14]. Within the compounds investigated, the hydroxamate of betulinic acid (BHA) was selected for additional studies because of its potent inhibition of hypoxia-inducing factor (HIF) prolyl-hydroxylases (PHDs) [14].

Under physiological conditions, the gastrointestinal tract is characterized by a steep oxygen gradient from the anaerobic lumen towards the highly vascularized submucosa, which generates so-called physiological hypoxia [15]; dysregulation of this oxygen gradient is observed in IBD [16]. A resulting imbalance between oxygen consumption and supply makes the inflamed intestinal mucosa severely hypoxic; with hypoxia being a common feature of IBD, hypoxia mimetic agents are potentially capable of having a positive effect. In line with this, barrier-protective mechanisms involve the critical participation of HIF, which has been linked to the production of trefoil factors [17], mucins [18], and β-defensins [19] as well as to the regulation of mucosal immune responses and the expression of tight junction proteins, such as claudin-1 [20]. Through the regulation of these factors, HIF provides a barrier-protective mechanism in intestinal disease, and additional studies have shown that PHD inhibition is indeed protective in murine models of colitis [21]. Initial studies have shown that two PHD inhibitors (dimethyloxalylglycine, DMOG [22], and FG-4497 [23]) could reduce inflammation in two widely used models of murine IBD, namely, dextran sulfate sodium (DSS)- and trinitrobenzene sulfonic acid (TNBS)-induced colitis. Since then, the anti-inflammatory activity of these compounds and their biological analogs, which have the same mechanism of action [24–26], has been confirmed in many studies. However, little is known about the activity of PHD inhibitors in intestinal fibrosis. It has been recently reported that PHD inhibition downregulates the expression of TGF-β1 in intestinal fibrosis [27], further supporting the development of new small molecules capable of inhibiting PHDs to serve as antifibrotic agents in the treatment of IBD.

MATERIALS AND METHODS

Compounds

Dimethyloxallyl glycine (DMOG) was purchased from Cayman Chemical (#CAY-71210, Cayman Chemical, Ann Arbor, MI, USA) and had a purity ≥98%. BAH (3β-hydroxylup-20(29)-en-28-oic acid hydroxamate) was synthesized as previously reported [14]. The chromatographic purity of BAH was 99.11%. Compounds were dissolved in a solution of ethanol:cremophor:saline (1:1:18).

Animals

All experiments were performed in strict accordance with the European Union (EU) and governmental regulations. Handling of animals was performed in compliance with the guidelines of animal care set by the EU guidelines 86/609/EEC and the Ethics Committee on Animal Experimentation at the University of Córdoba (UCO, Córdoba, Spain), which approved all the procedures described in this study (protocol number: 13–03–15–207). Measures to improve welfare and clinical status, as well as endpoint criteria, were established to minimize suffering and ensure animal welfare. Briefly, wet food pellets are placed on the bed cage when the animals begin to develop clinical signs to facilitate access to food and hydration. The following animals were purchased from Janvier Labs (Le Genest-Saint-Isle, France): male Balb/c mice for the TNBS model and male C56BL/6 mice for the DSS model. All animals were housed in animal facilities under the following controlled conditions: 12 h light/dark cycle; temperature 20 °C (±2 °C); 40%–50% relative humidity; and free access to standard food and water.

Induction and assessment of colitis

TNBS model. Presensitization with TNBS 1% was performed by shaving an area of skin on the back of the mice between the shoulders, which prevents the animal from licking the area (day 0). Then, animals were anesthetized by isoflurane inhalation, and TNBS was rectally administered weekly by a syringe attached to a 3.5 catheter; the TNBS was dissolved in ethanol to disrupt the intestinal barrier and enable the interaction of TNBS with colon tissue proteins. An increasing dose of TNBS was administered (0.75%: day 7, 1%: day 14, and 1.75%: day 21) to induce severe colitis disease [28]. Animals were administered BAH (20 mg/kg or 50 mg/kg) by oral gavage from day 7 to 23. The weights of the mice were recorded daily throughout the experiment. The animals were sacrificed at day 23, their colons were removed, and the length was measured.

DSS model. Drinking water was supplemented with 3% DSS (Mw: 36,000–50,000 Da; MP Biomedicals, Solon, OH, USA) ad libitum for 5 days followed by normal drinking water. Control healthy mice were allowed to drink only water. From days 5 to 20, animals were administered BAH (50 mg/kg) or a vehicle by oral gavage and DMOG via intraperitoneal injection; the concentration of DMOG was 8 mg per mouse, which is the standard concentration for this compound [22, 29, 30]. C56BL/6 mice developed colon fibrosis after DSS treatment [31]. Mice were sacrificed on day 20 of the experiment.

Histological analysis

After measuring their lengths, colons were opened longitudinally and cut into two halves; one was immediately frozen and kept at −80 °C for RT-PCR analysis, and the other was rolled with the mucosa outward into so-called Swiss rolls to allow microscopic examination of the entire length of the colon. The collected samples were transferred to 4% PFA buffer for an incubation of at least 24 h at 4 °C. Five-micrometer-thick sections of formalin-fixed paraffin-embedded colon samples were stained for hematoxylin and eosin or picrosirius red/fast green. Arbitrary histologic scoring was used to quantify colon damage. The score was calculated by modifying a previously described method [22] and assessing the percentage of tissue that presented each feature.

Immunohistochemistry analysis

For IHC analysis, colon sections (5 μm) were deparaffinized and boiled for 10 min in sodium citrate buffer (10 mM, pH 6.0). Endogenous peroxidase activity was inhibited by treatment with 3.3% hydrogen peroxide in methanol. The sections were blocked with 2.5% normal horse serum and then were incubated overnight at 4 °C in blocking buffer with the following primary antibodies: rat anti-F4/80 (1:50, #MCA497, Bio-Rad, Hercules, CA, USA), mouse anti-CD3 (1:50, #sc20047, Santa Cruz Biotechnology, CA, USA), rabbit anti-Muc-2 (1:100, #ab97386, Abcam, Cambridge, UK), rabbit anti-Cldn-1 (1:200, #ab15098, Abcam) and rabbit anti-Hif-1α (1:50, #ab179483, Abcam). To block nonspecific binding by endogenous mouse IgG rodent block M (#RBM961, Biocare Medical, Concord, CA, USA) was used prior to anti-CD3 antibody. Slides were incubated with ImmPRESS reagent (Vector Laboratories; Burlingame, CA, USA) for F4/80 and CD3 antibodies or with Vectastain Elite ABC HRP kit (#416411, Vector Laboratories) for Muc-2, Cldn-1 and Hif-1α proteins, which was followed by incubation with a secondary antibody (#A21537, Sigma). All samples were finally visualized with diaminobenzidine chromogen (Dako, Santa Clara, CA, USA), photographed and digitalized using a

Leica DFC420c camera and analyzed using ImageJ software (http://rsbweb.nih.gov/ij/).

Confocal microscopy analysis

For antigen retrieval, paraffin-embedded colon sections were deparaffinized and boiled for 10 min in sodium citrate buffer (10 mM, pH 6.0). The sections were washed three times in PBS-Triton X100-saponin (0.1%). Nonspecific antibody-binding sites were blocked by incubation for 1 h at room temperature with 3% bovine serum albumin (BSA). Next, the sections were incubated overnight at 4 °C in the following primary antibodies diluted in PBS with 3% BSA: rabbit anti-CD31 (1:100, #ab28364, Abcam, Cambridge, UK), rat anti-Tenascin (Tnc) (1:100, #MAB2138, RD system, Minneapolis, MN, USA), and mouse anti-α-Smooth muscle actin (α-SMA) conjugated to Alexa-488 (1:100, #53–9760–80, Thermo Fischer, Waltham, MA, USA). After extensive washing in PBS, slides were incubated with secondary antibodies for 1 h at room temperature in the dark. The immunoreactions were revealed using anti-rabbit Texas Red (1:100, #A-6399) and anti-rat Alexa 488 (1:100, #A-11006) obtained from Thermo Fischer Scientific. The tissue sections were then mounted with Vectashield Antifade Mounting Medium with DAPI (#H-1200, Vector Laboratories). All images were acquired using a spectral confocal laser-scanning microscope LSM710, (Zeiss, Jena, Germany) with a 20×/0.8 Plan-Apochromat lens, and quantification of 10–15 randomly chosen fields was performed using ImageJ software.

PCR arrays and quantitative reverse transcriptase-PCR

Total RNA was isolated from mouse colon tissue using QIAzol lysis reagent and an RNeasy Lipid mini kit (#74804, Qiagen, Hilden, Germany), and RNA was then purified with lithium chloride [32]. For the PCR array, an RT^2 Profiler PCR Array Mouse Fibrosis kit (#PAMM024ZD6, Qiagen) was used. One microgram of RNA was transcribed to generate cDNA using an RT^2 First-Strand Synthesis Kit (#330401, Qiagen) and analyzed using an RT^2 SYBR Green qPCR master mix (#330504, Qiagen). The fold change in gene expression was calculated using the $2^{-\Delta\Delta Ct}$ method, and five housekeeping genes were used for normalization following the manufacturer's instructions. Each array was performed with a pool of 4 mice. For qPCR assays, total RNA (1 µg) was retrotranscribed using an iScript cDNA Synthesis Kit (#1708891, Bio-Rad), and cDNA was analyzed by real-time PCR using iQTM SYBR Green Supermix (#1708880, Bio-Rad) and a CFX96 Real-time PCR Detection System (Bio-Rad). The *Gapdh* gene was used to standardize mRNA expression in each sample. Gene expression was quantified using the $2^{-\Delta\Delta Ct}$ method, and the percentage of relative expression against controls is shown. The primers used in this study are described in Table S1 (Supplementary Information).

Cell lines and reagents

The generation of NIH-3T3-EPO-luc was described previously [33], and Caco-2 cells were obtained from ATCC (Manassas, VA, USA). The cells were maintained at 37 °C in a humidified atmosphere containing 5% CO_2 in DMEM supplemented with 10% fetal bovine serum (FBS), 2 mM *L*-glutamine and 1% (*v*/*v*) penicillin/streptomycin (Sigma-Aldrich Co, St Louis, MO, USA). All other reagents were purchased from Sigma-Aldrich Co.

Trans-epithelial electrical resistance (TEER) analysis

Epithelial permeability was evaluated by trans-epithelial electrical resistance using a Millicell® ERS-2 (Electrical Resistance System, Millipore, MA, USA) on CaCo-2 monolayers. CaCo-2 cells were seeded at a density of 500,000 cells per well on polycarbonate inserts in 12-well transwell plates (6.5 mm diameter, 0.4 µm pore size) (#CLS3413–48EA, Sigma). Each insert was placed in a well of 12-well plates with 0.2 mL of medium in the apical chamber and 0.6 mL of medium in the basolateral chamber. CaCo-2 cells were treated with different concentrations of BAH for 24 h. Then, 200 µL of human peripheral blood mononuclear cell (PBMC) supernatant previously activated with phytohemagglutinin-M (PHA) for 48 h was added [34–36] for 30 min, and TEER measurements of each well were collected (vol/vol). The TEER values of the CaCo-2 monolayer were calculated by subtracting the blank resistance (background electrical resistance from an insert without cells including filter and medium) and multiplying that result by the effective growth area of the membrane (0.6 cm^2). The results are expressed as a percentage of epithelial disruption, taking 0% as the disruption in untreated cells.

Collagen retraction assay

NIH-3T3-EPO-luc fibroblasts were trypsinized, washed with PBS, and resuspended in complete medium at 500,000 cells/mL. Collagen gels were made containing a final concentration of 150,000 cells/mL and 1 mg/mL collagen I with or without the indicated concentrations of BAH or DMOG. Gels were digitally imaged upon setting (t 0) and at 12 h. The gel surface area was quantified in terms of pixel number using ImageJ. Relative changes in surface area are reported as a percentage of the original surface area.

Luciferase assay

For EPO-Luc transactivation as a marker of HIF stabilization, NIH-3T3-EPO-luc cells containing three copies of the HRE consensus sequence from the promoter of the erythropoietin gene fused to the luciferase gene were seeded in 96-well plates and stimulated as indicated. Luciferase activity was quantified using a dual-luciferase assay (#E1483, Promega, Madison, WI, USA) after 12 h of stimulation.

Western blotting and antibodies

After 6 h of treatment, cells were washed with PBS, and proteins were extracted in 50 µL of lysis buffer (50 mM Tris–HCl pH 7.5, 150 mM NaCl, 10% glycerol and 1% NP-40) supplemented with 10 mM NaF, 1 mM Na_3VO_4, 10 µg/mL leupeptin, 1 µg/mL pepstatin and aprotinin, and 1 µg/mL saturated PMSF. Fifty micrograms of protein was boiled at 95 °C in Laemmli buffer and electrophoresed in 8% SDS/PAGE gels. Separated proteins were transferred to PVDF membranes (20 V for 30 min) and blocked in TBS solution containing 0.1% Tween 20 and 5% nonfat dry milk for 1 h at room temperature. Immunodetection of specific proteins was carried out by incubation overnight at 4 °C with primary antibodies against murine HIF-1α (1:1000 dilution, #ab179483, Abcam) and β-actin (1:25.000 dilution, #ab49900, Abcam). After washing the membranes, a horseradish peroxidase-conjugated secondary antibody was added and detected by a chemiluminescence system (GE Healthcare Europe GmbH).

Pharmacokinetics

This study was performed by Pharmacology Discovery Services Taiwan (China), Ltd., which is a company in the Eurofins group. The experiment was performed in accordance with the Eurofins validation Standard Operating Procedure. Briefly, male ICR mice weighing 25 ± 5 g were provided by BioLasco Taiwan (China) (under Charles River Laboratories Licensee). The PK study was performed following administration of a single bolus of intravenous (IV) and oral (PO) BAH at 2 and 20 mg/kg, respectively. BAH was formulated in 5% DMSO/10% Solutol® HS15/85% saline at 0.4 mg/mL for IV and 1:1:18 ethanol:Cremophor® EL:saline at 2 mg/mL for PO administration. Plasma samples were collected at 3, 10, 60, 120, 240 and

480 min after IV administration and at 10, 30, 60, 120, 240, 360 and 480 min after PO treatment. The plasma samples were processed using acetonitrile precipitation and were analyzed by LC-MS/MS. A plasma calibration curve was generated. Aliquots of BAH-free plasma were spiked with the test compound at the specified concentration levels. The spiked plasma samples were processed together with the unknown plasma samples using the same procedure. The processed plasma samples were stored at −70 °C until LC-MS/MS analysis, at which time peak areas were recorded, and the concentrations of the test compound in the unknown plasma samples were determined using the respective calibration curve. The reportable linear range of the assay was determined, along with the lower limit of quantitation (LLQ). Plots of plasma concentration of the compound versus time were constructed. The fundamental pharmacokinetic parameters of each compound after IV ($t_{1/2}$, C_0, AUC_{last}, AUC_{Inf}, AUC_{Extr}, MRT, V_{ss}, and CL) and PO dosing (T_{max}, C_{max}, AUC_{last}, AUC_{Inf}, AUC/D, AUC_{Extr} and MRT) were obtained from the noncompartmental analysis (NCA) of the plasma data using WinNonlin. The bioavailability (F) was also calculated.

Statistical analysis

All in vitro data are expressed as the mean ± SD. One-way ANOVA followed by Tukey's or Dunnett's post hoc tests were used to determine the statistical significance. All in vivo data are expressed as the mean ± SEM. One-way or two-way analysis of variance (ANOVA) followed by Tukey's or Dunnett's post hoc tests were used to determine the statistical significance. The level of significance was set at $P < 0.05$. Statistical analyses were performed using GraphPad Prism version 6.00 (GraphPad, San Diego, CA, USA).

RESULTS

BAH induces collagen retraction and activates the HIF-1 pathway

BAH is a triterpenoid hydroxamate derived from betulinic acid (Fig. 1a) that is capable of inhibiting PHDs and stabilizing HIF [14]. PHD inhibitors improve wound healing and tissue remodeling; therefore, we first evaluated whether and to what extent BAH could induce similar responses. For this purpose, collagen gel contraction using NIH-3T3-EPO-Luc cells was used as a model of wound healing [23]. As shown in Fig. 1b, c,

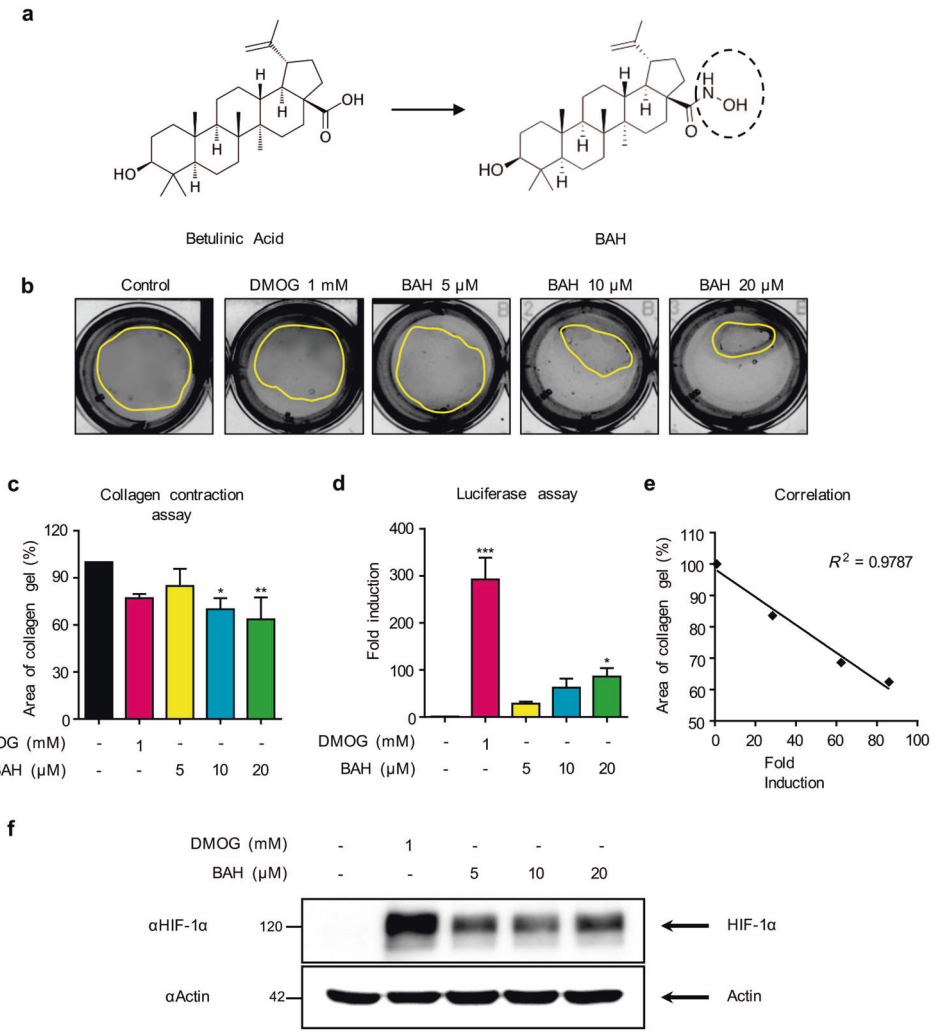

Fig. 1 Effect of BAH on collagen gel contraction and HIF activity. a Chemical structures of betulinic acid and BAH. **b** Images of contracted gel matrices in response to 12 h of BAH exposure. **c** Gel surface area quantified in terms of total pixel number using ImageJ. **d** NIH-3T3 fibroblasts stably transfected with a luciferase-HRE (NIH3T3-EPO-luc) were stimulated with the indicated concentrations of BAH or DMOG. **e** Correlation between HIF activity induced by BAH and collagen gel contraction. **f** HIF-1α protein expression in NIH-3T3-Epo-luc cells after 6 h of treatment with BAH and DMOG. Values are expressed as the mean ± SD. *$P < 0.05$ and ** $P < 0.01$ versus control group; significance was determined by one-way ANOVA followed by Dunnett's post hoc test.

exposure of fibroblast-embedded gels to BAH enhanced the contraction of collagen gels in a concentration-dependent manner, nicely paralleling the activation effect observed of the HIF pathway (Fig. 1d); the data are shown by a linear plot of HIF activity versus gel contraction. (Fig. 1e). In addition, BAH-induced HIF-1α protein expression in this cell line (Fig. 1f). These findings directly implicate HIF and BAH in tissue remodeling and wound contraction.

BAH alleviates colon inflammation and fibrosis induced by TNBS

After the first TNBS challenge (day 7), mice were administered BAH for 2 weeks. During this time, the control group showed a progressive body weight gain relative to the weight at day 0. In contrast, mice subjected to colitis showed transient weight loss for 2 days immediately after each TNBS treatment (Fig. 2a). At the endpoint (day 23), mice subjected to colitis induction (TNBS group) showed a significant loss in body weight compared with the control group. Mice treated with different doses of BAH also showed transient weight loss after each TNBS treatment, but weight loss was significantly mitigated over the entire follow-up period compared with that of the TNBS group. Two days after the last TNBS treatment (on day 23), mice were euthanized, and their colons were removed and evaluated macroscopically. Colons of TNBS-treated mice revealed a shortening in comparison with the control group, which was significantly prevented by treatment with BAH (Fig. 2b).

The beneficial effect of BAH was next confirmed by histological examination (Fig. 2c, d). In histopathological analysis of H&E-stained colon tissue, disruption of the epithelial barrier, transmural inflammation, ulcerations, loss of goblet cells, marked destruction in the crypts, and necrotic mucosal areas could be detected in the TNBS-treated mice but not in those treated with BAH. To evaluate the inflammatory process, IHC analysis was performed for $F4/80^+$ and $CD3^+$. Increased numbers of $F4/80^+$ and $CD3^+$ cells were accumulated at the mucosa of the lesion site in colonic tissues from TNBS-treated mice, and BAH treatment greatly reduced the number of infiltrating cells in colon tissues (Fig. 2c, d). To assess the fibrosis condition of the colon in TNBS mice, picrosirius red/fast green staining and tenascin C (Tnc) immunofluorescence staining were performed. High accumulation of both dyes, as well as of collagen and Tnc, was observed in the TNBS group compared to the control animals, but this accumulation could be alleviated by treatment with BAH. These results suggested that BAH can successfully ameliorate TNBS-induced colitis and fibrosis.

To further evaluate the antifibrotic activity of BAH in the TNBS model, a qPCR array of fibrosis-related genes was performed. Several genes related to inflammatory and fibrotic processes were dysregulated after the administration of TNBS compared to the levels observed in the control group, and this effect could be minimized by BAH at a 50 mg/kg dosage (Fig. 3a). These results were confirmed by qPCR analysis, which showed that the upregulated expression of *Tnc*, *Ccl3*, *Il-1β*, *Mmp-3*, *Mmp-8*, and *Timp1* was prevented by BAH treatment. Conversely, the expression of *Il-13* and *Mrc-1* was enhanced by BAH (Fig. 3b).

Rectal bleeding is one of the common features of IBD [37], and vascular damage in TNBS mice was therefore investigated by a morphometric analysis that measured blood vessel perimeter and area with CD31 as an endothelial marker. We observed that both parameters were significantly increased in the TNBS group compared with the control mice, but the parameters were recovered in mice treated with BAH (Fig. 4a, b).

Effect of BAH on epithelial barrier integrity

To further explore the effect of BAH in the colons of mice with TNBS-induced colitis, we first examined the mRNA levels of HIF-regulated genes associated with the integrity of the intestinal barrier, such as mucins and tight junction proteins [38]. In our experiments, TNBS markedly reduced the expression of these genes, but BAH could restore or even enhance the expression of *Itf, Muc-2, Muc-3, Cldn-1*, and *Zo-1* (Fig. 5a). IHC detection of Muc-2 and Cldn-1 confirmed these results at the protein level (Fig. 5b, c). Taken together, these observations indicate that BAH exerted a beneficial effect on TNBS-induced mucosa disruption. Since cytokines such as TNFα or IFNγ induce epithelial disruption [36], the effect of BAH on epithelial barrier disruption was additionally investigated in a more physiologically relevant model by incubating Caco-2 cells with different concentrations of BAH for 24 h; then, supernatants from PBMCs activated with PHA were added 30 min before TEER measurement. As shown in Fig. 5d, the supernatant of PHA-stimulated PBMCs contained a cocktail of pro-inflammatory cytokines and was able to induce clear epithelial disruption, which was significantly prevented in cells treated with BAH (Fig. 5d). Overall, all experimental data support the view that BAH has a positive effect on the integrity of the intestinal epithelial barrier.

BAH alleviates colon inflammation and fibrosis induced by DSS

Different animal models recapitulate different clinical and histological features of the types of IBD. Thus, those with TNBS-induced colitis are "CD-like" (associated with transmural inflammation and edema), while those with DSS colitis are "UC-like" (associated with epithelial disruption, focal lesions, and superficial inflammation) [28]. Previous studies have shown that the colonic damage induced by DSS is directly related to cellular infiltration in the intestinal mucosa [39]. For this reason, the protective effect of BAH on DSS-mediated colitis was additionally investigated by treating the animals for 2 weeks after receiving DSS for 5 days. Colons were processed for histological analysis by H&E and for F4/80 and CD3 staining (Fig. 6a, b). The colons of DSS mice showed destruction of colonic tissue, with histopathological changes in the mucosal, submucosal, muscular layer, and colonic wall. Furthermore, an increase in inflammatory cell numbers was observed in colonic tissue visualized by the staining of $F4/80^+$ and $CD3^+$ cells. In this model, DMOG was used as a positive control due to its protective effects on DSS-induced IBD [22]. BAH (50 mg/kg) and DMOG (8 mg/mouse) improved the histological score and diminished the number of inflammatory cells induced by DSS damage. Colon fibrosis was also alleviated by treatment with DMOG and BAH at the transcriptomic level, as shown by RT-PCR array (Fig. 7a) and confirmed by qPCR measurements of *Col1a2, Col3a1, Tnc* and *Timp-1* gene expression (Fig. 7b). In addition, colon tissues were also analyzed for the expression of fibrotic markers such as α-SMA and Tnc, and the results revealed that the increased expression in the DSS group was significantly reduced by treatment with both BAH and DMOG (Fig. 8a, b). To quantify the collagen content in the colon, picrosirius red/fast green staining was performed, and BAH significantly prevented its accumulation (Fig. 8c).

Rectally administered BAH does not prevent colon inflammation

Since sulfasalazine and mesalazine preparations have been used orally or rectally for many years for the treatment of IBD, we evaluated whether BAH could also exert anti-ulcerative activity via rectal delivery. As shown in Fig. 9a and compared with DMOG treatment and oral BAH administration, rectal administration of BAH did not improve the histological score or the collagen content, and no changes were observed in the features of DSS mice. These results strongly suggest that BAH acts systemically.

Pharmacokinetics and bioavailability of BAH

The pharmacokinetics of BAH were evaluated by a single-dose administration from two different formulations: IV at a concentration

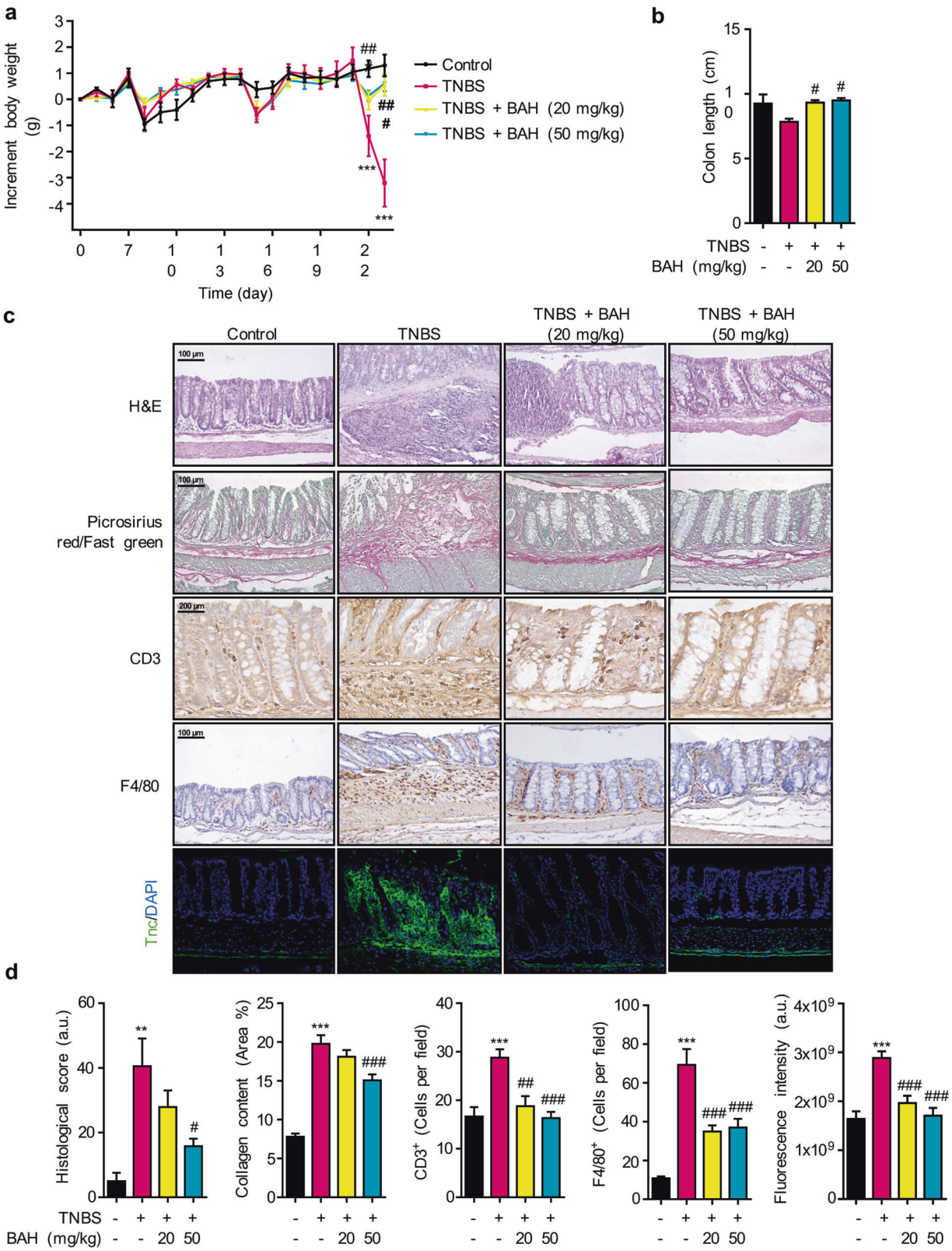

Fig. 2 BAH attenuates clinical severity, fibrosis and inflammatory-related biomarkers in the TNBS model. a BAH significantly ameliorated the decrease in body weight induced by TNBS. Significance was determined by two-way ANOVA followed by Tukey's post hoc test. **b** Colon length was measured at the time of sacrifice and was compared between groups. Significance was determined by one-way ANOVA followed by Dunnett's post hoc test. Panel **c** depicts histological sections stained with H&E or picrosirius red/fast green as well as images from immunohistochemistry experiments performed on macrophages (F4/80) or lymphocyte T (CD3) and from TNC immunofluorescence. Representative images are shown at the indicated magnification. **d** Quantification of different markers from panel **c**. All results are shown as the mean ± SEM ($n = 4$–10 animals per group), and significance was determined by one-way ANOVA followed by Tukey's post hoc test, with the exception of the histological score (Dunnett's test). $^{**}P < 0.01$ and $^{***}P < 0.001$ for TNBS + vehicle vs control + vehicle; $^{\#}P < 0.05$, $^{\#\#}P < 0.01$, and $^{\#\#\#}P < 0.001$ for TNBS + BAH vs TNBS + vehicle.

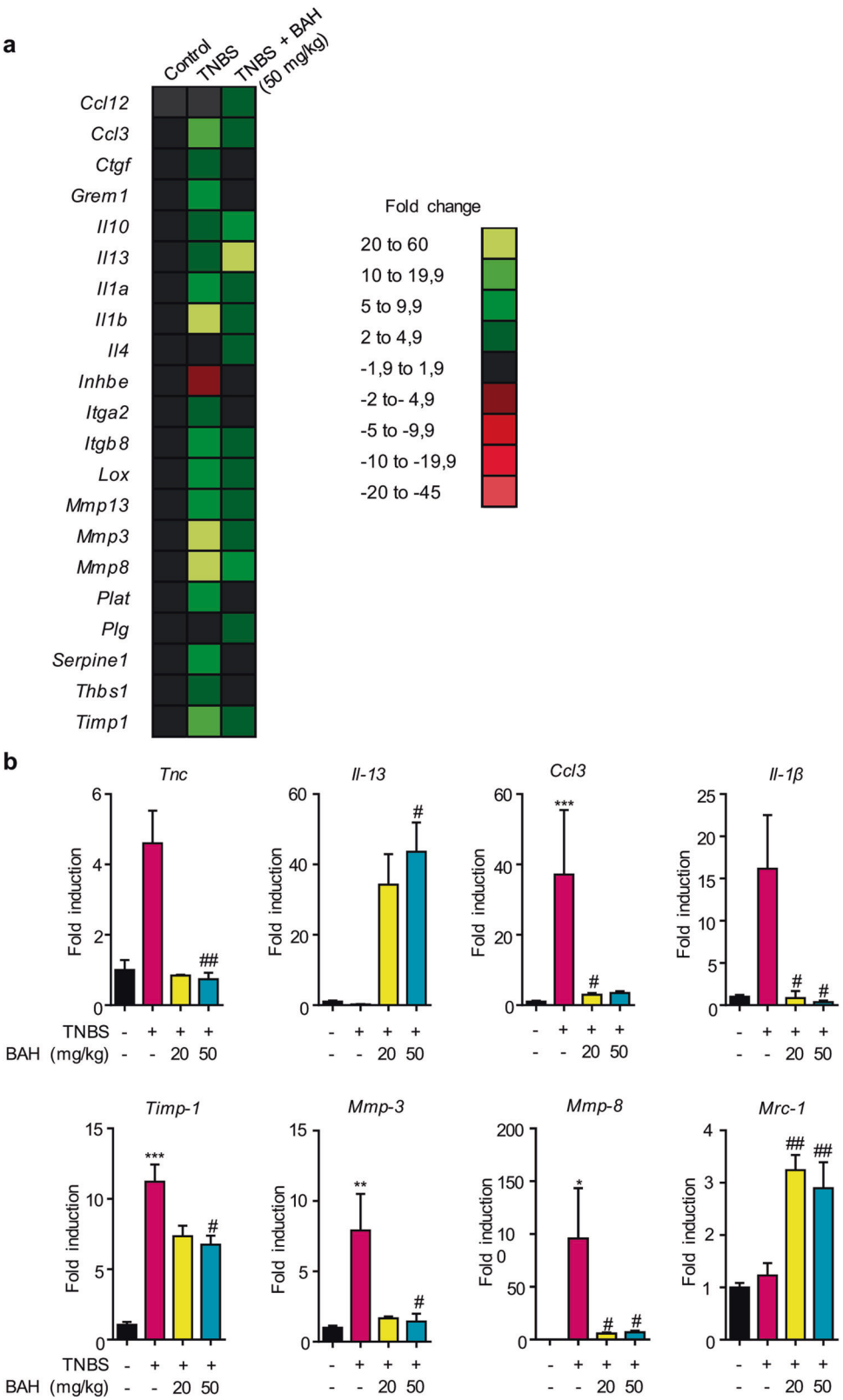

Fig. 3 BAH treatment normalized the expression of genes associated with fibrosis in the TNBS model. a RNA from colon tissue was used to determine the expression of genes involved in fibrosis by PCR array. Heat maps showed the significantly upregulated (green) or downregulated (red) genes in TNBS + vehicle or TNBS + BAH compared with control + vehicle. **b** The mRNA expression of fibrosis-related genes (*Tnc, Il-13, Timp-1, Il-1β, Ccl3, Mmp-3, Mmp-8*, and *Mrc-1*) was quantified by qPCR and normalized to the levels of *Gapdh*. Data represent the mean ± SEM, and significance was determined by one-way ANOVA followed by Dunnett's post hoc test. The results are expressed as the mean ± SEM ($n = 3$–7 animals per group) $^{*}P < 0.05$, $^{**}P < 0.01$, and $^{***}P < 0.001$ for TNBS + vehicle vs control + vehicle; $^{\#}P < 0.05$, and $^{\#\#}P < 0.01$ for TNBS + BAH vs TNBS + vehicle.

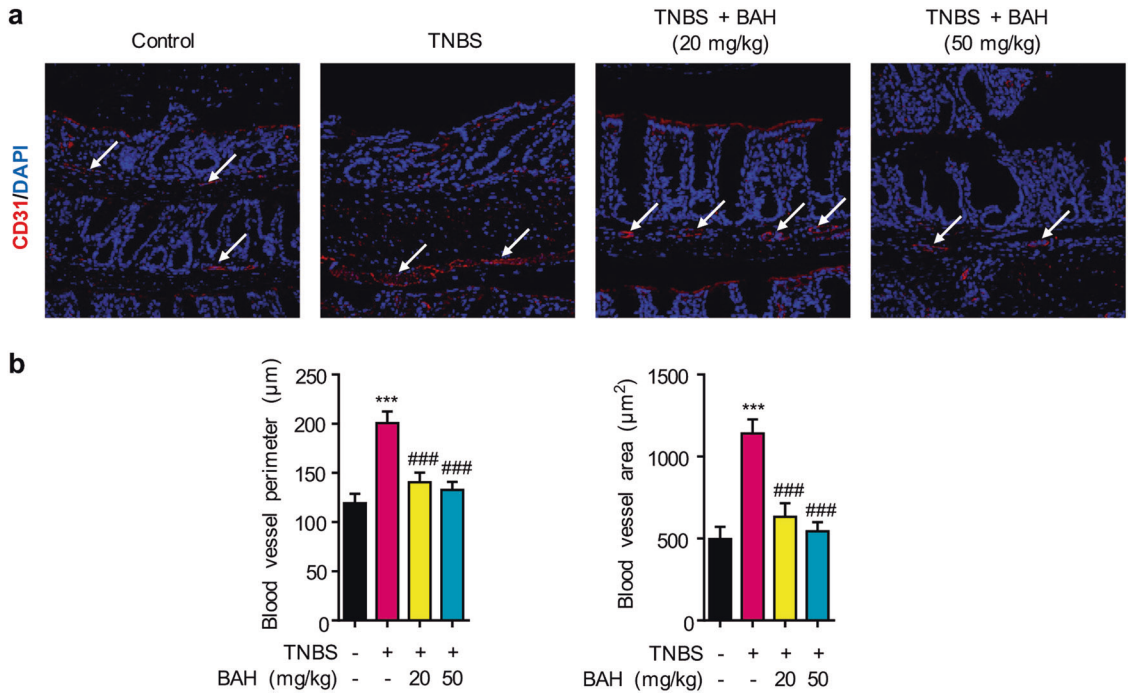

Fig. 4 Increase in blood vessel density and area were prevented by BAH treatment. a Representative confocal microscopy images (original magnification ×20) of vessels marked with CD31 (white arrows). **b** The quantification of the perimeter and area is shown as the mean ± SEM ($n = 4$ animals per group), and significance was determined by one-way ANOVA followed by Tukey's post hoc test. ***$P < 0.001$ for TNBS + vehicle vs control + vehicle; ###$P < 0.001$ TNBS + BAH vs TNBS + vehicle.

of 2 mg/kg and orally at 20 mg/kg. Mean plasma concentration-time curves are presented in Fig. 9b, and the main pharmacokinetic parameters are shown in Fig. 9c. After administration, a significant increase in BAH in the plasma concentration over time was observed in both routes. For IV administration, the plasma concentration at T_{max} (0.05 h) was 5659 ng/mL, and then it decreased rapidly until it reached nearly baseline levels. BAH was rapidly absorbed after oral administration, with a T_{max} of 0.5 h and C_{max} of 618 ng/mL during a detection time that extended for 8 h, and the bioavailability achieved was 7.6%.

Some critical toxicological and metabolic parameters were also investigated. By performing an in vitro test using the S9 fraction from human and rat livers, we found that BAH undergoes rapid intrinsic clearance in both species (Supplementary Fig. S1). Moreover, BAH did not significantly inhibit the activity of relevant cytochrome P450 isoforms (Supplementary Fig. S2), and it lacked in vitro hERG channel activity, suggesting a lack of drug interference and cardiotoxicity (Supplementary Fig. S3). BAH was also not genotoxic, as assessed by the Ames fluctuation test (Supplementary Fig. S4) and by comet assay (Supplementary Fig. S5). To evaluate potential off-target activities of BAH, in vitro pharmacological profiling of a panel of 68 different lead biological targets was carried out, and the results revealed a satisfactory safety profile (Supplementary Fig. S6). In addition, a metabolite identification study in human and rat microsomes ruled out the conversion of BAH into a single or a limited set of metabolites, ruling out the requirement of additional toxicological studies (Supplementary Fig. S7). Next, we decided to study Hif-1 expression in colon tissue (Fig. 9d). Immunochemistry of Hif-1 protein was performed in TNBS model samples and the results were that in control and BAH-treated mice the protein distribution was expected in healthy tissue, along the surface of the crypts, resembling the characteristics of the physiological hypoxia. However, mice that only received TNBS insults had a generalized expression of Hif-1 in the tissue confirming the inflammatory status of the colon.

DISCUSSION

Hypoxia-inducible factor (HIF), the major transcription factor that mediates the cellular response to hypoxia [40], is made up of two subunits: an oxygen-sensitive α (HIF-1α, HIF-2α, or HIF-3α) and a constitutive coactivator HIF-1β [41]. Under normoxic conditions, HIF-α mRNA is constitutively expressed, but HIF protein is rapidly and efficiently degraded by prolyl hydroxylases (PHDs) [42]. In the presence of sufficient levels of oxygen, PHDs hydroxylate specific proline residues in the oxygen-dependent degradation domain of HIF-α, which makes the protein a target of an E3 ubiquitin ligase (von Hippel-Lindau protein, VHL) that ubiquitinates HIF-α for proteasomal degradation. Under hypoxic conditions, the ability of PHDs to hydroxylate HIF-α is compromised, allowing HIF-α to accumulate, translocate to the nucleus, dimerize with HIF-1β, and activate the expression of over 200 genes involved in erythropoiesis, angiogenesis, intestinal barrier integrity, iron homeostasis, and glycolysis [43].

The potential of PHD inhibitors in the treatment of IBD has been documented in several in vivo models [22–24] that have associated their beneficial effects with the following combination of processes: restoring the intestinal barrier function secondary to inhibition of epithelial cell apoptosis by PHD1 [44], enhancing the expression of a battery of epithelial-specific barrier protective genes via the HIF pathway, and stimulating neutrophil apoptosis by PHD3 [45].

BAH is not an Fe^{2+} chelator and does not inhibit the enzymatic activity of PHDs; rather, it induces posttranslational modifications of PHD2, including dephosphorylation of serine 125, which is a modification known to stabilize HIF-1α [46]. Additional ongoing experiments are expected to further clarify

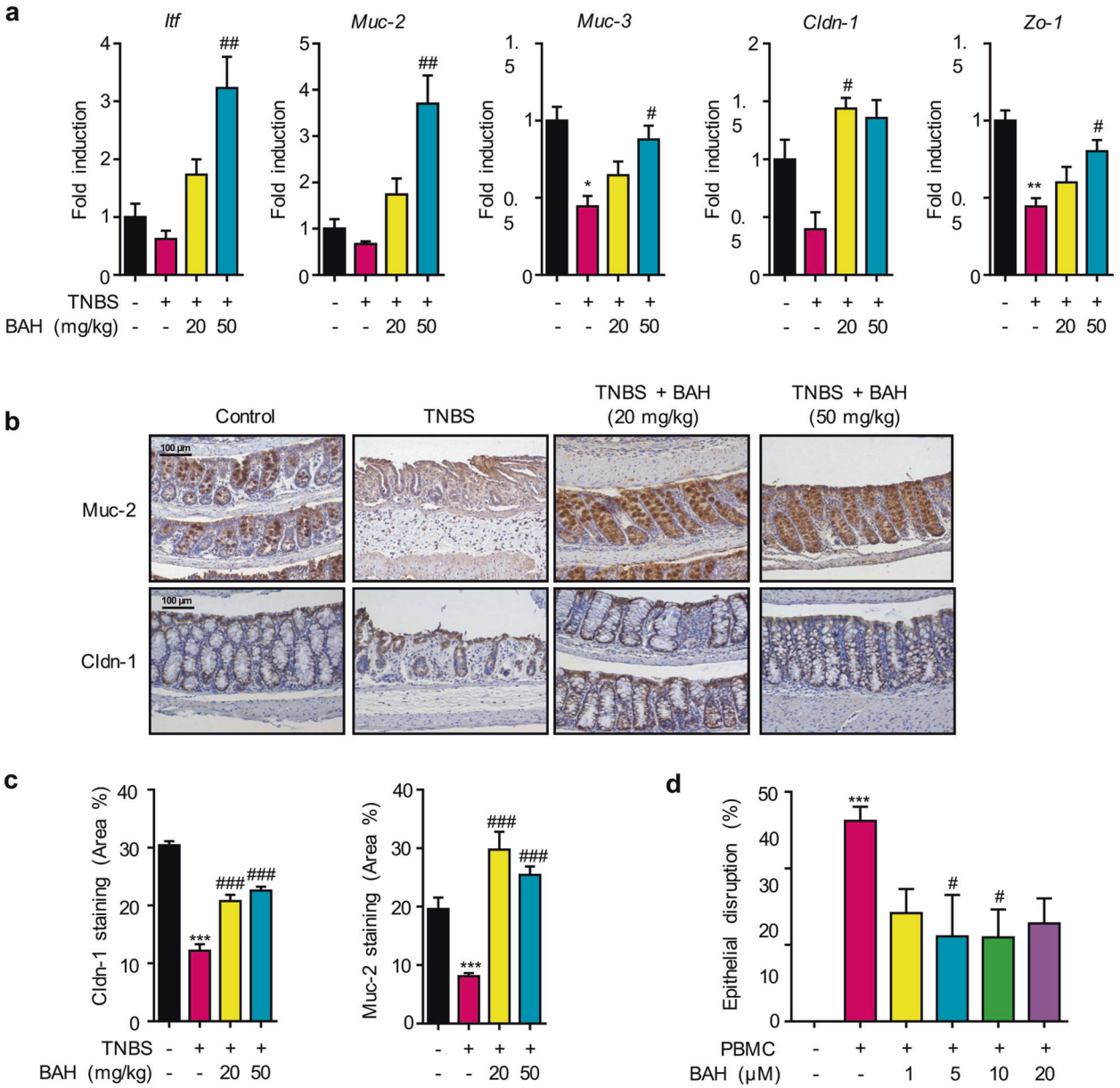

Fig. 5 BAH enhances intestinal epithelial barrier integrity. a A panel of genes related to epithelial barrier integrity was significantly increased in mice treated with the compound BAH. The quantification is shown as the mean ± SEM ($n = 3$–8 animals per group), and significance was determined by one-way ANOVA, which was followed by Dunnett's post hoc test. **b** Images show immunostaining of colon sections for the mucin-specific marker Muc-2 and the tight junction protein Claudin-1 at an original magnification of 20×; their quantification (**c**) is shown as the mean ± SEM ($n = 4$ animals per group), and significance was determined by one-way ANOVA followed by Tukey's post hoc test. $^{*}P < 0.05$, $^{**}P < 0.01$, and $^{***}P < 0.001$ for TNBS + vehicle vs control + vehicle; $^{\#}P < 0.05$, $^{\#\#}P < 0.01$, and $^{\#\#\#}P < 0.001$ for TNBS + BAH vs TNBS + vehicle. **d** BAH treatment protected against epithelial disruption promoted by PBMCs in the Caco-2 cell line. Data represent the mean ± SD ($n = 5$). $^{***}P < 0.001$ for PBMC-treated cells vs control; $^{\#}P < 0.05$ for BAH-treated cells vs PBMC-treated cells (one-way ANOVA followed by Tukey's post hoc test).

the molecular details of the activity and selectivity of BAH as a PHD inhibitor, but it was still important to validate the activity in preclinical models of disease. For this purpose, we used murine models of colon inflammation and fibrosis that mimic human UC (DSS model) and CD (TNBS model), respectively. In the TNBS model, the colon toxin was administered weekly to Balb/c mice, inducing chronic colitis with inflammation and fibrosis [47]. In the DSS model, C57BL/6 mice were used to study colitis, since in this strain, the acute disease does not resolve after stopping DSS treatment; rather, it progresses into severe and chronic fibrosis [31]. Our results showed that, in both models, oral treatment with BAH ameliorated not only colon fibrosis but also inflammation.

It is well known that HIF can modulate innate and acquired immune responses, and therefore, an anti-inflammatory activity of BAH was expected in both IBD models [21, 48]. HIF has cell type-specific roles, which have a profound impact on immune cell gene expression and downstream effector function. For example, HIF has a key role in the regulation of lifespan and apoptosis of neutrophils [49], regulates M1 and M2 polarization in macrophages [50], and modulates survival and interferon synthesis in dendritic cells [51]. Similarly, HIF is

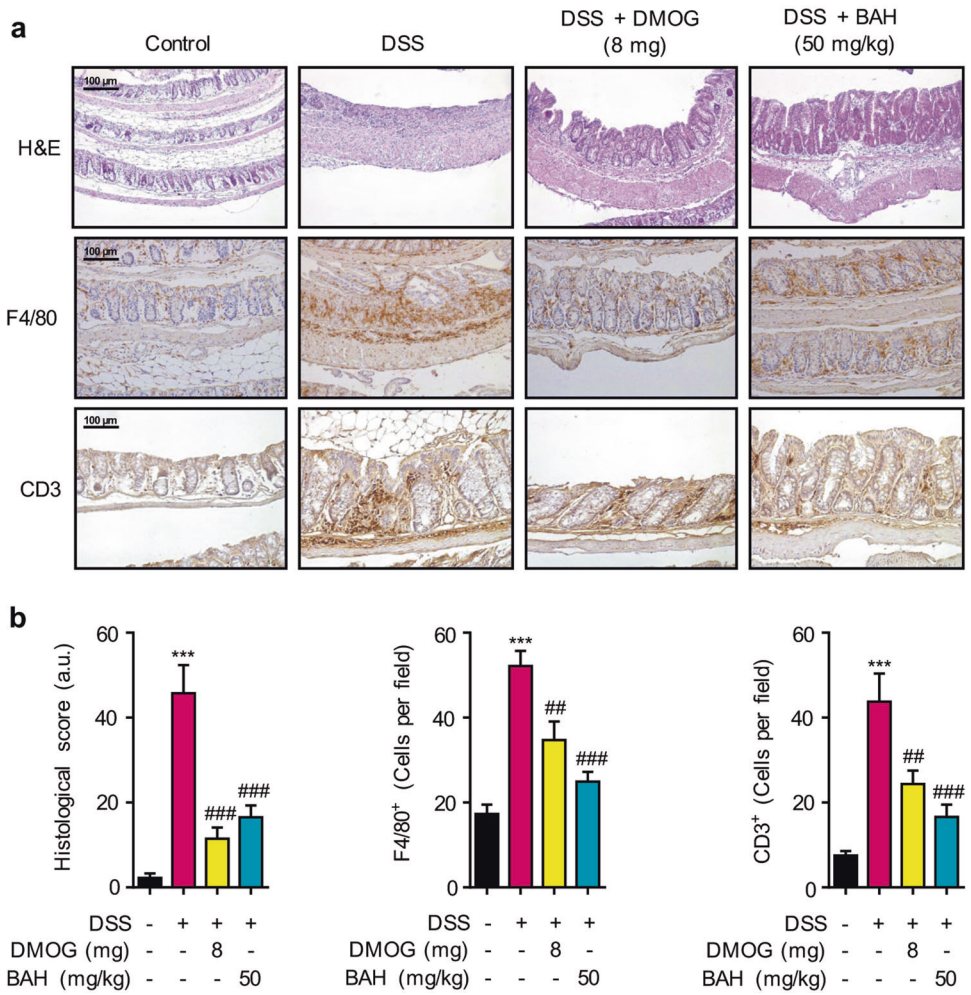

Fig. 6 BAH significantly reduces inflammation and preserves epithelial structure in the colon of DSS animals. a Representative images of H&E staining and macrophage (F4/80) and lymphocyte (CD3) infiltration in colon sections [original magnification (×20)]. **b** BAH and DMOG treatments improved the histological score and the number of inflammatory cells present in colon tissues. Quantification is shown as the mean ± SEM ($n = 4$–7 animals per group), and significance was determined by one-way ANOVA followed by Tukey's post hoc test. $^{***}P < 0.001$ for DSS + vehicle vs control + vehicle; $^{\#\#}P < 0.01$, and $^{\#\#\#}P < 0.001$ for DSS + BAH or DSS + DMOG vs DSS + vehicle.

important for the regulation of not only the survival and differentiation of T-cells but also their proliferation and antitumor capacity [52], while in B cells, HIF also regulates survival as well as antibody production [53]. In both models, a general improvement in immune infiltrates, including a reduction in the number of macrophages ($F4/80^+$) and lymphocytes ($CD3^+$), was observed. In addition, the expression of proinflammatory genes induced in the TNBS model, such as *Ccl3* and *Il-1β*, decreased after BAH treatment. Conversely, *Il-13* and its target gene *Mrc-1* exhibited increased expression in mice treated with BAH, while their levels remained unchanged in TNBS-treated and control mice.

Contradictory roles have been reported for IL-13 and colitis, with studies generally showing a link between this cytokine and fibrosis; however, in some cases, anti-inflammatory effects have also been described [54]. Thus, in a TNBS model, IL-13 could induce fibrosis in a TGF-β-dependent manner [47], but other reports based on the same colitis model suggested that IL-13 could be beneficial for chronic colitis [55]. In this model, spontaneous amelioration of chronic inflammation was shown to be critically dependent on IL-13 activation of STAT6, which was followed by inactivation of glycogen synthase kinase-3β and ultimately resulting in a switch from IL-17 to IL-10 production by immune cells. This spontaneous recovery in the TNBS model could be enhanced by oral administration of BAH. Alternatively, it is also conceivable that BAH targets downstream signaling of IL-13, thus explaining why, despite elevated levels of this cytokine, fibrosis was mainly prevented in the TNBS model. For instance, we found an increase in *Mrc-1* gene expression, which is associated with the anti-inflammatory macrophage M2 phenotype. Further research to elucidate the role of M2 macrophages in the therapeutic activity of BAH is warranted.

Mucosal intestinal surfaces are lined by epithelial cells that provide a selective barrier between biologic surfaces, preventing the free mixing of luminal antigenic material with the underlying tissues and the trigger of an immunological response. In line with this, our in vitro and in vivo results demonstrated the protective effect of BAH on barrier integrity, as shown by TEER measurements and the induction of genes and proteins such as Muc-2, Muc-3, Itf, Zo-1, and Cldn-1. It is likely that the protection mediated by BAH in the epithelium could cause a decrease in the introduction of luminal material into the organism, which would decrease activation of the immune system, inflammation and

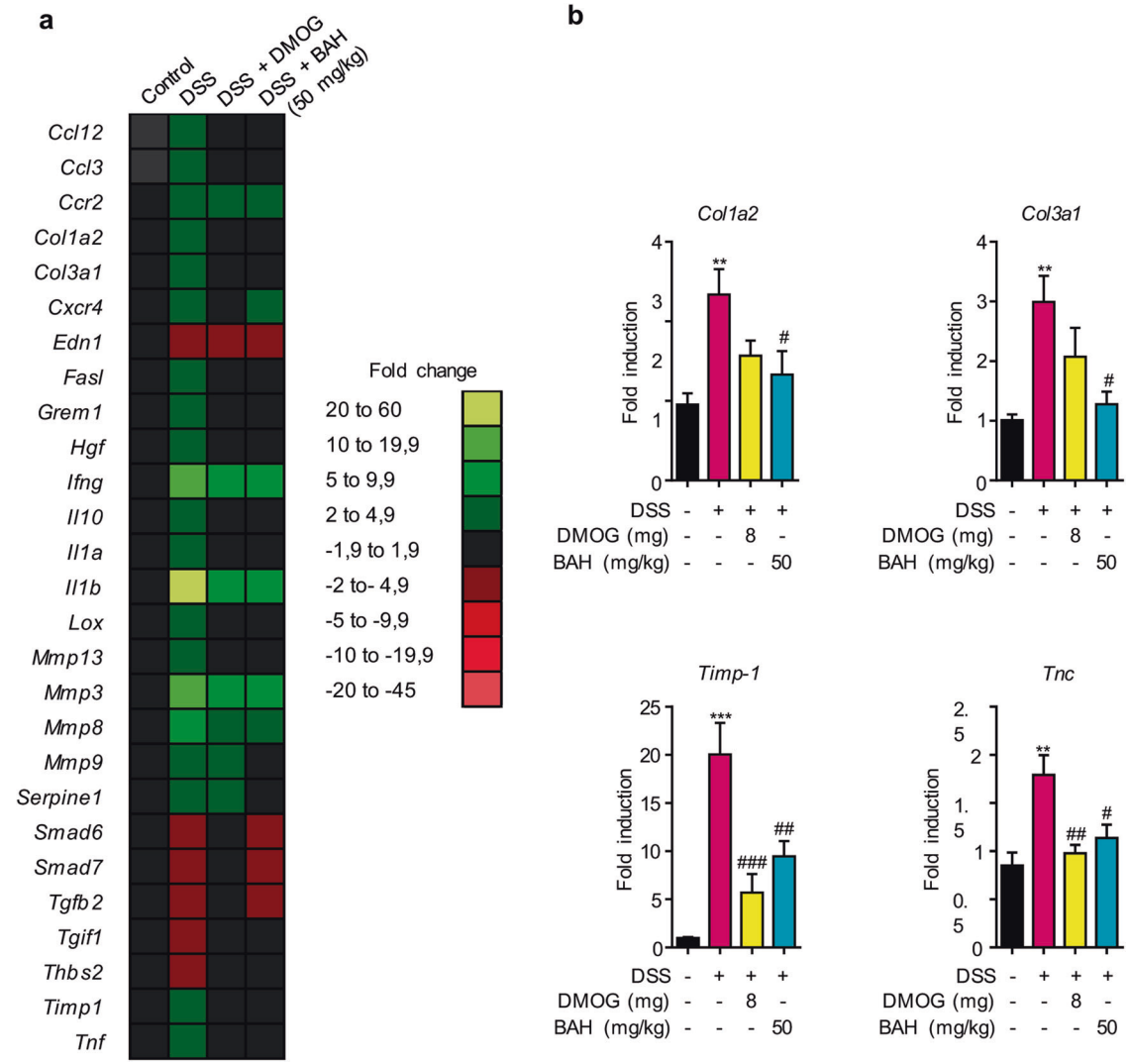

Fig. 7 BAH treatment normalized the expression of genes associated with fibrosis in the DSS model. a RNA from colon tissue was used to determine the expression of genes involved in fibrosis by PCR array. Heat maps showed the significantly upregulated (green) or downregulated (red) genes in DSS + vehicle, DSS + BAH or DSS + DMOG compared with control + vehicle. **b** The mRNA expression of fibrosis-related genes (*Col1a2, Col3a1, Timp-1*, and *Tnc*) was quantified by qPCR and normalized to levels of *Gapdh*. Data represent the mean ± SEM, and significance was determined by one-way ANOVA followed by Tukey's post hoc test. $^{**}P < 0.01$, and $^{***}P < 0.001$ for DSS + vehicle vs control + vehicle; $^{\#}P < 0.05$, $^{\#\#}P < 0.01$, and $^{\#\#\#}P < 0.001$ for DSS + BAH or DSS + DMOG vs DSS + vehicle.

fibrosis. This mucosal protection could be the result of compensatory mechanisms of barrier protection at the epithelial level, as well as of a promotion of restitution by wound healing associated with BAH.

Over their lifetime, a large number of CD patients suffer from clinically apparent intestinal obstruction due to fibrostenosis [56] with surgery being the only treatment available. Our study demonstrates that oral administration of BAH greatly ameliorates the increase in fibrotic-related markers at the RNA level in both TNBS and DSS mice, resulting in downregulated expression of genes such as *Col1a2, Col3a1, Tnc, Timp-1, Mmp-3*, and *Mmp-8* and alleviated expression of collagen, TNC and α-SMA at the protein level. These results could be the consequence of a reduced colonic inflammatory state associated with improved epithelial barrier integrity and the switch produced by *Il-13*. BAH could diminish fibrosis in colon tissue by acting through different pathways that eventually induce a general improvement of the different parameters of the disease. It is important to mention that in both colitis models, treatment with BAH significantly decreased the levels of Tnc, a protein not only related to fibrosis but also to cancer and metastasis [57, 58]. In particular, it has been established that patients with IBD have an increased risk of developing colorectal cancer or colitis-associated colorectal cancer [59, 60]. Moreover, several studies have also reported that upregulated expression of Tnc is present in IBD and colon cancer patients [61, 62], suggesting that the BAH-induced reduction of Tnc levels could also be potentially beneficial in other aspects of the disease not addressed in this study. In addition, it has been reported that BAH exhibits anticancer activity in vitro, although the mechanism of action for this activity has not been investigated [63, 64].

The low oral bioavailability of formulated BAH suggests major fecal excretion and accumulation in the colon. However, the lack of an effect of BAH delivered intrarectally indicates that either the compound is degraded by the colonic flora or that BAH is acting at the systemic level. Interestingly, several small molecules acting at the systemic level are currently being

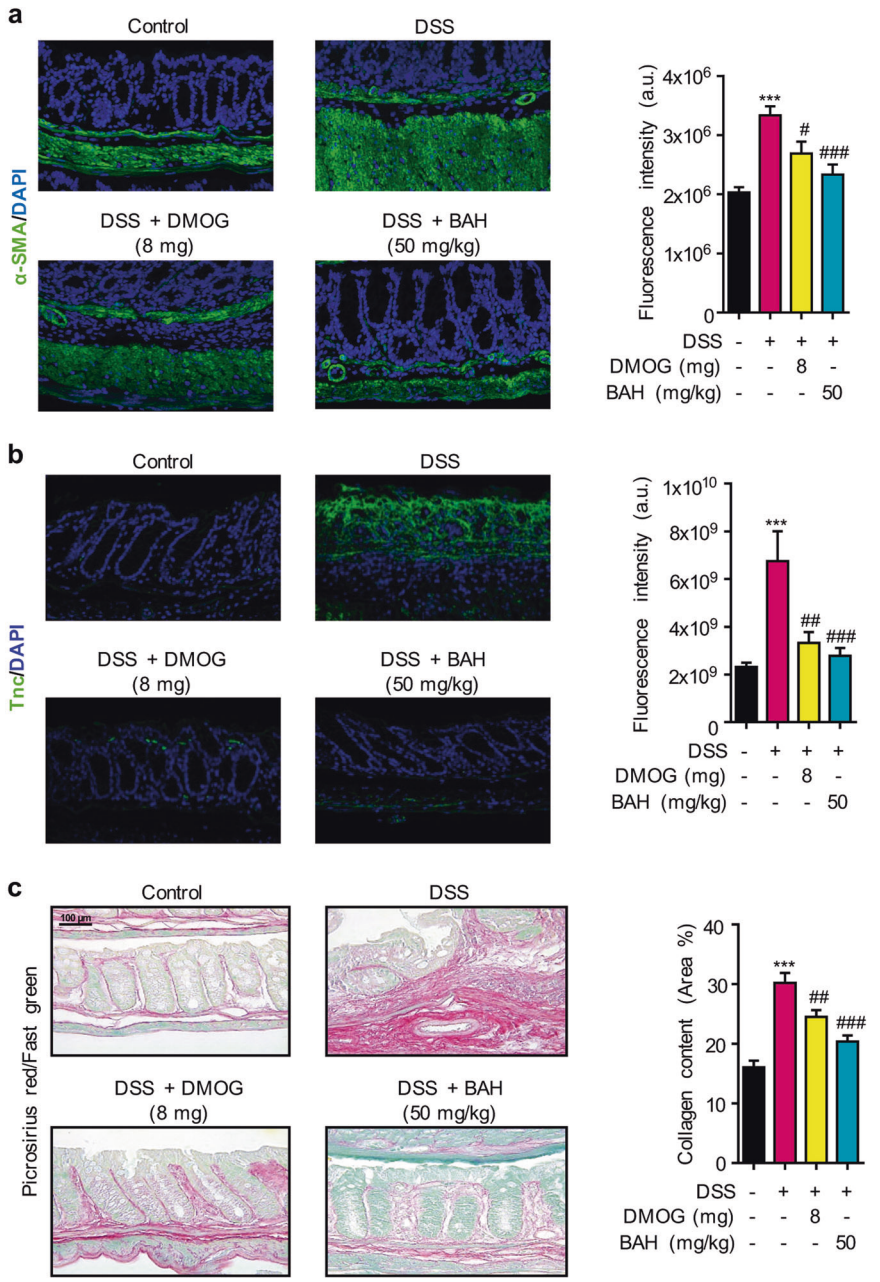

Fig. 8 BAH prevents colon fibrosis in the DSS model. a Representative confocal microscopy images of smooth muscle cells (α-SMA, green fluorescence) in colon sections and their quantification. **b** Immunofluorescence labeling of TNC (green fluorescence) in the control, DSS + vehicle, DSS + DMOG and DSS + BAH groups is shown. **c** Representative images of Picrosirius Red/Fast Green staining (left panel). Comparison of the collagen content among the experimental groups (right panel). The original magnification of all images is ×20. The quantification is shown as the mean ± SEM ($n = 6–8$ animals per group), and significance was determined by one-way ANOVA followed by Tukey's post hoc test. $^{***}P < 0.001$ for DSS + vehicle vs control + vehicle; $^{\#}P < 0.05$, $^{\#\#}P < 0.01$, and $^{\#\#\#}P < 0.001$ for DSS + BAH or DSS + DMOG vs DSS + vehicle.

developed for the oral treatment of IBD [65]. Similar to AJM300, an oral antagonist of α4-integrin can reduce inflammation by blocking leukocyte trafficking [66]. We do not yet know the exact target tissue(s) involved in the systemic activity of BAH, and off-target effects are the major drawbacks facing drug candidates with systemic activity [29, 67]. We, therefore, tested BAH with a panel of 68 potential drug targets, none of which was affected at therapeutic concentrations. This, along with the lack of mutagenic activity, suggests that BAH may have a safe profile useful in pharmacological development.

In summary, the hypoxia mimetic triterpenoid derivative BAH could provide protection on the chronic phases of mucosal inflammation and fibrosis in two different murine models of IBD, improving immune infiltrates, reducing the number of macrophages ($F4/80^{+}$) and lymphocytes ($CD3^{+}$), and selectively inducing or repressing the expression of various genes involved in tissue maintenance and inflammation. These observations associated with a promising PK and toxicological profile qualify BAH for additional development as a potential treatment for the management of colon fibrosis in IBD.

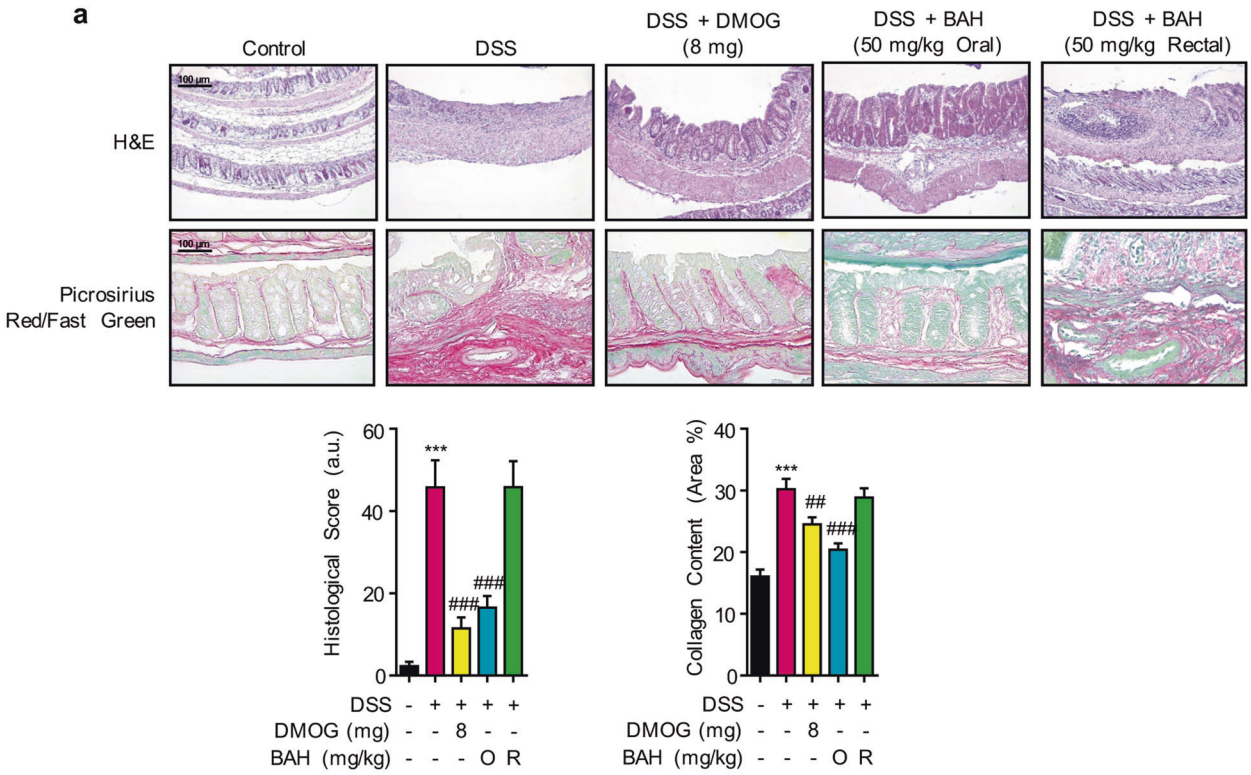

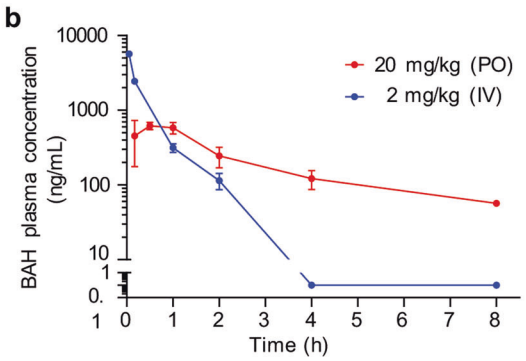

c

Route	T_{max} (h)	C_{max} (ng/mL)	AUC_{inf} (h·ng/mL)	F (%)
Intravenous	0.05	5659	2240	
Oral	0.5	618	1894	7.6

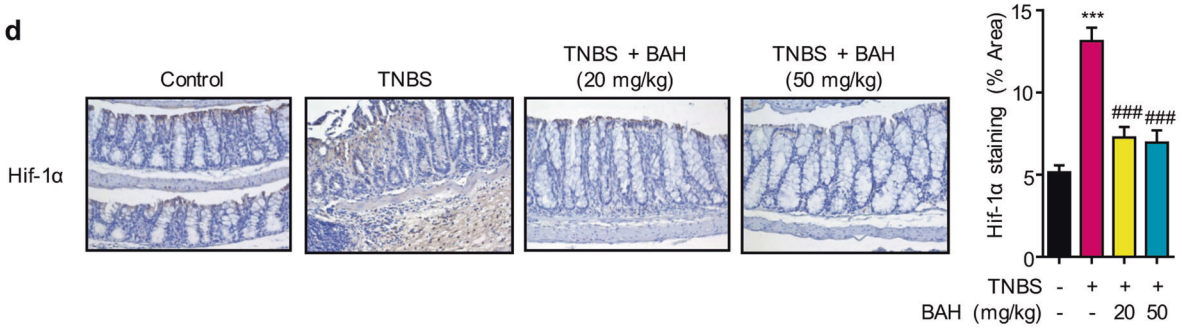

Fig. 9 BAH exerts its functions systemically but not intrarectally. a BAH improved the histological score and collagen content when administered by oral gavage but not when administered rectally (original magnification ×20). The quantification is shown as the mean ± SEM ($n = 6–8$ animals per group), and significance was determined by one-way ANOVA followed by Tukey's post hoc test. $^{***}P < 0.001$ for DSS + vehicle vs control + vehicle; $^{\#\#}P < 0.01$, and $^{\#\#\#}P < 0.001$ for DSS + BAH or DSS + DMOG vs DSS + vehicle. **b** Mean plasma concentration-time profile and main pharmacokinetic parameters (**c**) of BAH after PO (20 mg/kg) and IV (2 mg/kg) administration in mice. The results are expressed as the mean ± SD ($n = 3$ animals per group). **d** BAH treatment normalized the expression of Hif-1α protein in colon during TNBS insult (original magnification ×20). Data represent the mean ± SEM, and significance was determined by one-way ANOVA followed by the Tukey's post-hoc test. Results are expressed as mean ± SEM ($n = 4$ animals per group). $^{***}P < 0.001$ TNBS + Vehicle vs Control + Vehicle; $^{\#\#\#}P < 0.001$ TNBS + BAH vs TNBS + Vehicle.

ACKNOWLEDGEMENTS

We thank Carmen-Cabrero for revising the manuscript. This work was supported by grants RTC-2017–6109–1 (EM) from the Ministry of the Economy and Competition (MINECO) and was co-financed with European Union FEDER funds. This work was also partially supported by Emerald Health Biotechnology España (Cordoba, Spain).

AUTHOR CONTRIBUTIONS

MEP, AGM, and JDUB performed in vivo experiments. MEP, BP, and JAC performed in vitro experiments; AM and GA synthesized BAH; and EM and MAC managed and designed the overall study. MEP and EM wrote the manuscript. All the authors approved the final manuscript.

ADDITIONAL INFORMATION

The online version of this article (https://doi.org/10.1038/s41401-020-0497-0) contains supplementary material, which is available to authorized users.

Competing interests: MEP, AGM, and JDUB are employees of Emerald Health Biotechnology. EM is a member of the Scientific Advisory Boards of Emerald Health Biotechnology. None of the authors have conflicts of interest. GA, AM, and EM have submitted a PCT with the publication number WO2018/069086A.

Ethics approval and consent to participate: All experiments with laboratory animals were conducted according to European guidelines (directive 2010/63/EU), and the Ethics Committee on Animal Experimentation at the University of Cordoba (Cordoba, Spain) that approved all the procedures described in this study (protocol number: 13–03–15–207).

REFERENCES

1. Liverani E, Scaioli E, Digby RJ, Bellanova M, Belluzzi A. How to predict clinical relapse in inflammatory bowel disease patients. World J Gastroenterol. 2016;22:1017–33.
2. Rieder F, Fiocchi C, Rogler G. Mechanisms, management, and treatment of fibrosis in patients with inflammatory bowel diseases. Gastroenterology. 2017;152:340–50 e346.
3. Koutroubakis IE, Ramos-Rivers C, Regueiro M, Koutroumpakis E, Click B, Schoen RE, et al. Persistent or recurrent anemia is associated with severe and disabling inflammatory bowel disease. Clin Gastroenterol Hepatol. 2015;13:1760–6.
4. Lawrance IC, Maxwell L, Doe W. Inflammation location, but not type, determines the increase in TGF-beta1 and IGF-1 expression and collagen deposition in IBD intestine. Inflamm Bowel Dis. 2001;7:16–26.
5. Silverstein MD, Loftus EV, Sandborn WJ, Tremaine WJ, Feagan BG, Nietert PJ, et al. Clinical course and costs of care for Crohn's disease: Markov model analysis of a population-based cohort. Gastroenterology. 1999;117:49–57.
6. Rieder F, Fiocchi C. Intestinal fibrosis in IBD-a dynamic, multifactorial process. Nat Rev Gastroenterol Hepatol. 2009;6:228–35.
7. Podolsky DK. Inflammatory bowel disease. N Engl J Med. 2002;347:417–29.
8. Annese V, Duricova D, Gower-Rousseau C, Jess T, Langholz E. Impact of new treatments on hospitalisation, surgery, infection, and mortality in IBD: a Focus Paper by the Epidemiology Committee of ECCO. J Crohns Colitis. 2016;10:216–25.
9. Billiet T, Rutgeerts P, Ferrante M, Van Assche G, Vermeire S. Targeting TNF-alpha for the treatment of inflammatory bowel disease. Expert Opin Biol Ther. 2014;14:75–101.
10. Kalra J, Lingaraju MC, Mathesh K, Kumar D, Parida S, Singh TU, et al. Betulinic acid alleviates dextran sulfate sodium-induced colitis and visceral pain in mice. Naunyn Schmiedebergs Arch Pharmacol. 2018;391:285–97.
11. Bildziukevich U, Ozdemir Z, Wimmer Z. Recent achievements in medicinal and supramolecular chemistry of betulinic acid and its derivatives (double dagger). Molecules. 2019;24:3546.
12. Saneja A, Arora D, Kumar R, Dubey RD, Panda AK, Gupta PN. Therapeutic applications of betulinic acid nanoformulations. Ann NY Acad Sci. 2018;1421:5–18.
13. Rios JL, Manez S. New pharmacological opportunities for betulinic acid. Planta Med. 2018;84:8–19.
14. Minassi A, Rogati F, Cruz C, Prados ME, Galera N, Jinenez C, et al. Triterpenoid hydroxamates as HIF prolyl hydrolase inhibitors. J Nat Prod. 2018;81:2235–43.
15. Taylor CT, Colgan SP. Hypoxia and gastrointestinal disease. J Mol Med (Berl). 2007;85:1295–1300.
16. Cummins EP, Crean D. Hypoxia and inflammatory bowel disease. Microbes Infect. 2017;19:210–21.
17. Furuta GT, Turner JR, Taylor CT, Hershberg RM, Comerford K, Narravula S, et al. Hypoxia-inducible factor 1-dependent induction of intestinal trefoil factor protects barrier function during hypoxia. J Exp Med. 2001;193:1027–34.
18. Louis NA, Hamilton KE, Canny G, Shekels LL, Ho SB, Colgan SP. Selective induction of mucin-3 by hypoxia in intestinal epithelia. J Cell Biochem. 2006;99:1616–27.
19. Kelly CJ, Glover LE, Campbell EL, Kominsky DJ, Ehrentraut SF, Bowers BE, et al. Fundamental role for HIF-1alpha in constitutive expression of human beta defensin-1. Mucosal Immunol. 2013;6:1110–8.
20. Saeedi BJ, Kao DJ, Kitzenberg DA, Dobrinskikh E, Schwisow KD, Masterson JC, et al. HIF-dependent regulation of claudin-1 is central to intestinal epithelial tight junction integrity. Mol Biol Cell. 2015;26:2252–62.
21. Taylor CT, Doherty G, Fallon PG, Cummins EP. Hypoxia-dependent regulation of inflammatory pathways in immune cells. J Clin Invest. 2016;126:3716–24.
22. Cummins EP, Seeballuck F, Keely SJ, Mangan NE, Callanan JJ, Fallon PG, et al. The hydroxylase inhibitor dimethyloxalylglycine is protective in a murine model of colitis. Gastroenterology. 2008;134:156–65.
23. Robinson A, Keely S, Karhausen J, Gerich ME, Furuta GT, Colgan SP. Mucosal protection by hypoxia-inducible factor prolyl hydroxylase inhibition. Gastroenterology. 2008;134:145–55.
24. Marks E, Goggins BJ, Cardona J, Cole S, Minahan K, Mateer S, et al. Oral delivery of prolyl hydroxylase inhibitor: AKB-4924 promotes localized mucosal healing in a mouse model of colitis. Inflamm Bowel Dis. 2015;21:267–75.
25. Gupta R, Chaudhary AR, Shah BN, Jadhav AV, Zambad SP, Gupta RC, et al. Therapeutic treatment with a novel hypoxia-inducible factor hydroxylase inhibitor (TRC160334) ameliorates murine colitis. Clin Exp Gastroenterol. 2014;7:13–23.
26. Jeong S, Park H, Hong S, Yum S, Kim W, Jung Y. Lipophilic modification enhances anti-colitic properties of rosmarinic acid by potentiating its HIF-prolyl hydroxylases inhibitory activity. Eur J Pharmacol. 2015;747:114–22.
27. Manresa MC, Tambuwala MM, Radhakrishnan P, Harnoss JM, Brown E, Cavadas MA, et al. Hydroxylase inhibition regulates inflammation-induced intestinal fibrosis through the suppression of ERK-mediated TGF-beta1 signaling. [corrected]. Am J Physiol Gastrointest Liver Physiol. 2016;311:G1076–90.
28. Wirtz S, Popp V, Kindermann M, Gerlach K, Weigmann B, Fichtner-Feigl S, et al. Chemically induced mouse models of acute and chronic intestinal inflammation. Nat Protoc. 2017;12:1295–309.
29. Tambuwala MM, Manresa MC, Cummins EP, Aversa V, Coulter IS, Taylor CT. Targeted delivery of the hydroxylase inhibitor DMOG provides enhanced efficacy with reduced systemic exposure in a murine model of colitis. J Control Release. 2015;217:221–7.
30. Taniguchi CM, Miao YR, Diep AN, Wu C, Rankin EB, Atwood TF, et al. PHD inhibition mitigates and protects against radiation-induced gastrointestinal toxicity via HIF2. Sci Transl Med. 2014;6:236ra264.
31. Melgar S, Karlsson A, Michaelsson E. Acute colitis induced by dextran sulfate sodium progresses to chronicity in C57BL/6 but not in BALB/c mice: correlation between symptoms and inflammation. Am J Physiol Gastrointest Liver Physiol. 2005;288:G1328–38.
32. Viennois E, Tahsin A, Merlin D. Purification of total RNA from DSS-treated murine tissue via lithium chloride precipitation. Bio Protoc. 2018;8:e2829.
33. Safari A, Parsaei H, Zamani A, Pourabbas B. Semi-automatic algorithm for estimating Cobb Angle. J Biomed Phys Eng. 2019;9:317–26.
34. Bruewer M, Luegering A, Kucharzik T, Parkos CA, Madara JL, Hopkins AM, et al. Proinflammatory cytokines disrupt epithelial barrier function by apoptosis-independent mechanisms. J Immunol. 2003;171:6164–72.
35. Capaldo CT, Nusrat A. Cytokine regulation of tight junctions. Biochim Biophys Acta. 2009;1788:864–71.
36. Al-Sadi R, Boivin M, Ma T. Mechanism of cytokine modulation of epithelial tight junction barrier. Front Biosci. 2009;14:2765–78.
37. Farmer RG. Lower gastrointestinal bleeding in inflammatory bowel disease. Gastroenterol Jpn. 1991;26:93–100.
38. Glover LE, Colgan SP. Epithelial barrier regulation by Hypoxia-Inducible Factor. Ann Am Thorac Soc. 2017;14:S233–6.
39. Oh SY, Cho KA, Kang JL, Kim KH, Woo SY. Comparison of experimental mouse models of inflammatory bowel disease. Int J Mol Med. 2014;33:333–40.
40. Semenza GL, Wang GL. A nuclear factor induced by hypoxia via de novo protein synthesis binds to the human erythropoietin gene enhancer at a site required for transcriptional activation. Mol Cell Biol. 1992;12:5447–54.
41. Wang GL, Jiang BH, Rue EA, Semenza GL. Hypoxia-inducible factor 1 is a basic-helix-loop-helix-PAS heterodimer regulated by cellular O_2 tension. Proc Natl Acad Sci USA. 1995;92:5510–4.
42. Jaakkola P, Mole DR, Tian YM, Wilson MI, Gielbert J, Gaskell SJ, et al. Targeting of HIF-alpha to the von Hippel-Lindau ubiquitylation complex by O_2-regulated prolyl hydroxylation. Science. 2001;292:468–72.
43. Ortiz-Barahona A, Villar D, Pescador N, Amigo J, del Peso L. Genome-wide identification of hypoxia-inducible factor binding sites and target genes by a probabilistic model integrating transcription-profiling data and in silico binding site prediction. Nucleic Acids Res. 2010;38:2332–45.

44. Tambuwala MM, Cummins EP, Lenihan CR, Kiss J, Stauch M, Scholz CC, et al. Loss of prolyl hydroxylase-1 protects against colitis through reduced epithelial cell apoptosis and increased barrier function. Gastroenterology. 2010;139:2093–101.
45. Walmsley SR, Chilvers ER, Thompson AA, Vaughan K, Marriott HM, Parker LC, et al. Prolyl hydroxylase 3 (PHD3) is essential for hypoxic regulation of neutrophilic inflammation in humans and mice. J Clin Invest. 2011;121:1053–63.
46. Di Conza G, Trusso Cafarello S, Loroch S, Mennerich D, Deschoemaeker S, Di Matteo M, et al. The mTOR and PP2A pathways regulate PHD2 phosphorylation to fine-tune HIF1alpha levels and colorectal cancer cell survival under hypoxia. Cell Rep. 2017;18:1699–712.
47. Fichtner-Feigl S, Fuss IJ, Young CA, Watanabe T, Geissler EK, Schlitt HJ, et al. Induction of IL-13 triggers TGF-beta1-dependent tissue fibrosis in chronic 2,4,6-trinitrobenzene sulfonic acid colitis. J Immunol. 2007;178:5859–70.
48. Cummins EP, Keogh CE, Crean D, Taylor CT. The role of HIF in immunity and inflammation. Mol Asp Med. 2016;47–48:24–34.
49. Harris AJ, Thompson AR, Whyte MK, Walmsley SR. HIF-mediated innate immune responses: cell signaling and therapeutic implications. Hypoxia (Auckl). 2014;2:47–58.
50. Lin N, Simon MC. Hypoxia-inducible factors: key regulators of myeloid cells during inflammation. J Clin Invest. 2016;126:3661–71.
51. Wobben R, Husecken Y, Lodewick C, Gibbert K, Fandrey J, Winning S. Role of hypoxia inducible factor-1alpha for interferon synthesis in mouse dendritic cells. Biol Chem. 2013;394:495–505.
52. Tyrakis PA, Palazon A, Macias D, Lee KL, Phan AT, Velica P, et al. S-2-hydroxyglutarate regulates $CD8^+$ T-lymphocyte fate. Nature. 2016;540:236–41.
53. Cho SH, Raybuck AL, Stengel K, Wei M, Beck TC, Volanakis E, et al. Germinal centre hypoxia and regulation of antibody qualities by a hypoxia response system. Nature. 2016;537:234–8.
54. Giuffrida P, Caprioli F, Facciotti F, Di Sabatino A. The role of interleukin-13 in chronic inflammatory intestinal disorders. Autoimmun Rev. 2019;18:549–55.
55. Fichtner-Feigl S, Kesselring R, Martin M, Obermeier F, Ruemmele P, Kitani A, et al. IL-13 orchestrates resolution of chronic intestinal inflammation via phosphorylation of glycogen synthase kinase-3beta. J Immunol. 2014;192:3969–80.
56. Rieder F. Managing intestinal fibrosis in patients with inflammatory bowel disease. Gastroenterol Hepatol (N. Y). 2018;14:120–2.
57. Sun Z, Schwenzer A, Rupp T, Murdamoothoo D, Vegliante R, Lefebvre O, et al. Tenascin-C promotes tumor cell migration and metastasis through Integrin alpha9beta1-mediated YAP inhibition. Cancer Res. 2018;78:950–61.
58. Lowy CM, Oskarsson T. Tenascin C in metastasis: a view from the invasive front. Cell Adh Migr. 2015;9:112–24.
59. Stidham RW, Higgins PDR. Colorectal cancer in inflammatory bowel disease. Clin Colon Rectal Surg. 2018;31:168–78.
60. Keller DS, Windsor A, Cohen R, Chand M. Colorectal cancer in inflammatory bowel disease: review of the evidence. Tech Coloproctol. 2019;23:3–13.
61. Yang Z, Zhang C, Qi W, Cui C, Cui Y, Xuan Y. Tenascin-C as a prognostic determinant of colorectal cancer through induction of epithelial-to-mesenchymal transition and proliferation. Exp Mol Pathol. 2018;105:216–22.
62. Zhou M, Li M, Liang X, Zhang Y, Huang H, Feng Y, et al. The Significance of serum S100A9 and TNC levels as biomarkers in colorectal cancer. J Cancer. 2019;10:5315–23.
63. Wiemann J, Heller L, Perl V, Kluge R, Strohl D, Csuk R. Betulinic acid derived hydroxamates and betulin derived carbamates are interesting scaffolds for the synthesis of novel cytotoxic compounds. Eur J Med Chem. 2015;106:194–210.
64. Wiemann J, Heller L, Csuk R. Targeting cancer cells with oleanolic and ursolic acid derived hydroxamates. Bioorg Med Chem Lett. 2016;26:907–9.
65. White JR, Phillips F, Monaghan T, Fateen W, Samuel S, Ghosh S, et al. Review article: novel oral-targeted therapies in inflammatory bowel disease. Aliment Pharmacol Ther. 2018;47:1610–22.
66. Fukase H, Kajioka T, Oikawa I, Ikeda N, Furuie H. AJM300, a novel oral antagonist of alpha4-integrin, sustains an increase in circulating lymphocytes: a randomised controlled trial in healthy male subjects. Br J Clin Pharmacol. 2020;86:591–600.
67. Fukata N, Uchida K, Kusuda T, Koyabu M, Miyoshi H, Fukui T, et al. The effective therapy of cyclosporine A with drug delivery system in experimental colitis. J Drug Target. 2011;19:458–67.